Pure & Appl. Chem., Vol. 64, No. 4, pp. 545–574, 1992.
Printed in Great Britain.

INTERNATIONAL UNION OF PURE
AND APPLIED CHEMISTRY

ANALYTICAL CHEMISTRY DIVISION
COMMISSION ON MICROCHEMICAL TECHNIQUES AND TRACE ANALYSIS*
SUBCOMMITTEE ON SURFACE ANALYSIS†

PREPARATION AND CERTIFICATION OF ION-IMPLANTED REFERENCE MATERIALS: A CRITICAL REVIEW

(Technical Report)

Prepared for publication by

WERNER H. GRIES

Research Institute of the Deutsche Bundespost, FTZ, POB 5000, D-6100 Darmstadt, FRG

*Membership of the Commission during the period (1983–1989) when this report was prepared was as follows:

Chairman: 1983–89 B. Griepink (Netherlands); *Secretary*: 1983–85 A. Townshend (UK); 1985–89 D. E. Wells (UK); *Titular Members*: K. Biemann (USA, 1983–89); W. H. Gries (FRG, 1985–89); E. Jackwerth (FRG, 1983–87); A. Lamotte (France, 1983–87); M. J.-F. Leroy (France, 1987–89); Z. Marczenko (Poland, 1983–89); D. G. Westmoreland (USA, 1987–89); Yu. A. Zolotov (USSR, 1983–87); *Associate Members*: K. Ballschmiter (FRG, 1983–87); K. Beyermann (FRG, 1983–85); R. Dams (Belgium, 1983–89); K. Fuwa (Japan, 1983–89); M. Morita (Japan, 1987–89); H. Muntau (Italy, 1985–89); J. M. Ottaway (UK, 1983–85); M. J. Pellin (USA, 1985–89); L. Reutergårdh (Sweden, 1987–89); B. D. Sawicka (Canada, 1987–89); E. A. Schweikert (USA, 1987–89); G. Scilla (USA, 1987–89); B. Ya. Spivakov (USSR, 1985–89); A. Townshend (UK, 1983–85); G. Tölg (FRG, 1983–85); D. E. Wells (UK, 1983–85); W. Wegscheider (Austria, 1987–89); D. G. Westmoreland (USA, 1983–87); *National Representatives*: R. Gijbels (Belgium, 1983–89); H. Thoma (Brazil, 1983–85); Zhe-ming Ni (Chinese Chemical Society, 1985–89); J. Janák (Czechoslovakia, 1983–85); M. J.-F. Leroy (France, 1983–87); Z. Horváth (Hungary, 1983–85); M. Sankar Das (India, 1983–85); S. M. Khopkar (India, 1985–89); R. C. H. Hsia (Malaysia, 1983–85); A. D. Campbell (New Zealand, 1983–89); B. Salbu (Norway, 1983–85); W. Kemula (Poland, 1983–85); C. Camara (Spain, 1987–89); A. Cedergren (Sweden, 1983–87); W. Frech (Sweden, 1987–89); S. Güçer (Turkey, 1987–89); J. M. Ottaway (UK, 1985–87); L. Ebdon (UK, 1987–89); E. A. Terent'eva (USSR, 1985–87); R. V. Golovnya (USSR, 1987–89).

†Membership of the Subcommittee: 1983–1989

Chairman: 1983–87 M. Grasserbauer (Austria); 1987–89 W. H. Gries (FRG); *Members*: J. Dufour (France, 1985–89); W. Eckstein (FRG, 1987–89); S. Gaarenstroom (USA, 1987–89); B. J. Garrison (USA, 1987–89); M. Grasserbauer (Austria, 1987–89); R. J. Ch. Hagemann (France, 1983–89); W. H. Gries (FRG, 1983–87); K. Heinrich (USA, 1983–85); K. L. Loening (USA, 1987–89); G. H. Morrison (USA, 1983–89); M. J. Pellin (USA, 1985–89); C. J. Powell (USA, 1987–89); L. Rehn (USA, 1987–89); B. D. Sawicka (Canada, 1987–89); E. A. Schweikert (USA, 1987–89); G. Scilla (USA, 1987–89); C. Sénémaud (France, 1983–89); W. B. Sonneveld (Netherlands, 1987–89); C. Stander (RSA, 1987–89).

Preparation and certification of ion-implanted reference materials: A critical review (Technical Report)

Abstract - The preparation and certification of ion-implanted reference materials is critically evaluated and information is provided for the analyst to specify and query conditions of ion implantation and certification. The information consists of (1) discussion of ion implantation generally, of quantitative ion implantation in particular, and of the differences between theoretical, as-implanted, and as-measured depth distributions, and (2) data on sputtering yields, limiting dose densities for quantitative ion implantation, concentrations at the distribution maximum and at the surface, for implantants (analytes) and host materials with atomic numbers between 10 and 80, for implantation energies between 10 and 300 keV. A nomenclature is introduced which provides for the special requirements of certification of ion-implanted reference materials.

CONTENTS

1. INTRODUCTION

Reference materials prepared by ion implantation consist of two basic components, the **host** and the **analyte**. The host is a solid material which should ideally be single-phased, void-free and flat-surfaced. Into this material a known quantity of the analyte is injected by means of a beam of energetic (keV) ions of the analyte which is directed at the surface of the host. The injection is performed in a heavy ion accelerator capable of delivering a high-purity ion beam of the analyte to the host. These accelerators essentially are oversized mass spectrometers of the magnetic type, known as **ion implanters**. Hence, the beam of analyte is monoisotopic.

At the host, the analyte ions collide with the host atoms, when they are scattered and slowed down to a stop. The average range of the ions in the host depends primarily on the kinetic energy of the analyte ions, on the mass ratio

of the atoms of analyte and host, on the angle of ion incidence, and on the crystallographic state of the host (ion channeling!).

The ions of a given energy come to rest at different depths such that the concentration of the implanted analyte is non-uniform with depth; in the absence of ion channeling the concentration changes smoothly from a non-zero value at the surface to a broad single-peaked maximum and further to zero at the maximum penetration depth, as shown schematically in Fig. 1. By proper choice of the dose density (defined below and in Appendix 1) the peak concentration can be made to assume any desired value between a few percent and the intrinsic level. This depth distribution of the analyte is usually asymmetrical (skew) w.r.t. the concentration maximum; the rather frequent reports of (symmetrical) Gaussian concentration profiles are over-simplifications. The lateral distribution of the analyte is rendered uniform (to various degrees of perfection) by appropriate scanning of the analyte beam over the surface of the host.

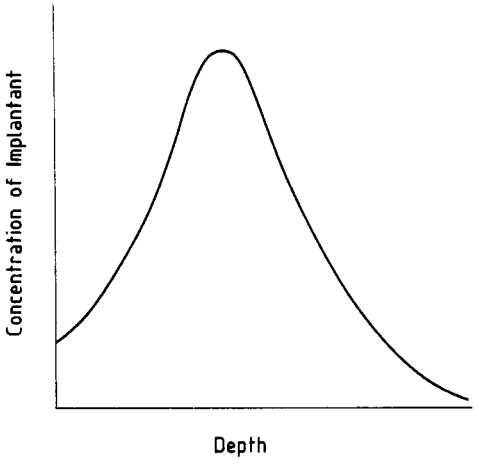

Fig. 1: The depth profile of concentration of an ion-implanted analyte (schematic).

The implanted region of the host can become a **reference material** if "one or more of the properties (of this region) are sufficiently well established to be used for the calibration of an apparatus, the assessment of a measurement method or for assigning values to materials" (ISO Guide 30-1981). It can become a **certified reference material** if "one or more (of its) property values are certified by a technically valid procedure, accompanied by or traceable to a certificate or other documentation which is issued by a certifying body" (ISO Guide 30-1981). Such properties of interest here are the **retained dose**, the **retained dose density**, and the **concentration vs depth profile**. Each of these properties is certifiable (to various degrees of accuracy). The exact chemical and physical states of the implanted analyte are difficult to determine.

The retained dose can be determined either from the integral over time of the ionic beam current incident on the host, or by post-implantation measurement (using any other technically valid procedure). The former of these two procedures is relatively simple, is applicable in all cases where the mass number of the analyte is not lower than that of the major component of the host (explained below), is capable of high accuracy (if a certain dose density is not exceeded), but is prone to hidden errors; it is restricted to as-implanted (i.e. unannealed) specimens. The second procedure is less simple generally, is costly, is usually less accurate, yet as prone to error, and it is likely to fail in a large number of cases; it is not restricted to as-implanted specimens.

The hidden errors in the first procedure are quantified and accounted for under the carefully controlled conditions known as **quantitative ion implantation**. This is the procedure of choice for the preparation and part-certification of primary reference materials with semiconductor hosts in an international collaboration (Versailles Project on Advanced Materials and Standards, VAMAS)

(ref. 1). For certification of the retained dose density, quantitative ion implantation is combined with at least one additional post-implantation determination of this quantity. Quantitative ion implantation is described and critically evaluated here in an effort to improve the transparency of the many-faceted process of preparation and certification of ion-implanted reference materials. Shortcomings in commercially available ion-implanted reference materials will be apparent therefrom.

Existing problems can be traced in part to an imprecision of the **vocabulary** in use. This tends to mask the errors referred to above. For instance, the term 'dose' is used to denote a quantity of analyte incident on as well as retained by the host, and then either as a total quantity or per square centimetre of surface. Dose in the latter sense, called 'dose density' here, has often been termed 'fluence', despite the existence of a different ISO definition for the latter term ('fluence' has sometimes been used wrongly also by the present author). There are also marked differences in the nomenclature used by analysts and other specialists; e.g. implanter technologists direct *ions* at a *target*, which to the semiconductor technologist constitutes *impurity* doping of a *wafer* (say) and to the analyst is the introduction of an *analyte* into a *host* material. In this report, the terms analyte and host are used as well as the terms **target** and **implantant** (i.e. 'that which is to be implanted'). 'Analyte in an ion beam' (as used above) is a misnomer generally; henceforth, it is replaced by implantant or **nominal constituent**, where 'nominal' refers to the practice of naming an ion beam for its major *intentional* constituent. Recommendations are made for a standardized terminology (Appendix 1) which is designed to avoid existing imprecision and to expose the true relationship between the physical quantities which the terms are meant to represent.

The use of ion implantation for analytical purposes has been proposed by different authors at different times. While used by some simply as a convenient method for injecting an analyte into a host without relying on in-situ ion dosimetry for a determination of the quantity injected (ref. 2), others have taken advantage of in-situ ion dosimetry as a convenient means of measurement (ref. 3). As a rule, though, standard ion dosimetry in technological ion implanters does not provide more than a reasonable approximation to the true value of the retained dose density; a statement which is supported by the round-robin data presented in Appendix 2. According to the records available, the first report of investigations into the special conditions for quantitative ion implantation was presented at a conference in 1970 (ref. 4). The first author of that paper has stayed with the subject (refs. 1, 5-18). A brief overview is provided by refs. 13 and 15, a detailed treatment in refs. 9 and 10. Since no comparable treatment of quantitative ion implantation has appeared in the literature, the present report has to rely heavily on this one author and collaborators for references.

The application of quantitative ion implantation for the preparation and certification of reference materials has received a new impetus from the VAMAS collaboration referred to above. The concept proposed for VAMAS is sketched in section 7.

2. ESSENTIAL INFORMATION ON ION IMPLANTERS

Fig. 2 pertains. In the fifties and sixties, research type ion implanters were used by nuclear physicists for the separation of radionuclides produced by nuclear reactions. For this purpose, irradiated material containing the isotope of interest was evaporated and ionized in an ion source, the ions were accelerated to several 10^4 eV energy, focussed into a pencil beam, separated into constituent isotopic beams by passage through a magnetic field, and the isotope of interest was intercepted by a collector foil or disc, known as target, placed in the focal plane of the implanter. The machines developed for this task, known as 'electromagnetic isotope separators', were capable of high mass resolution ($M/\Delta M$ up to 2500; M is the nominal relative mass, and ΔM is the full width at half maximum of the intensity profile of the beam measured in units of relative mass at M), the total beam current was about 0.1 mA.

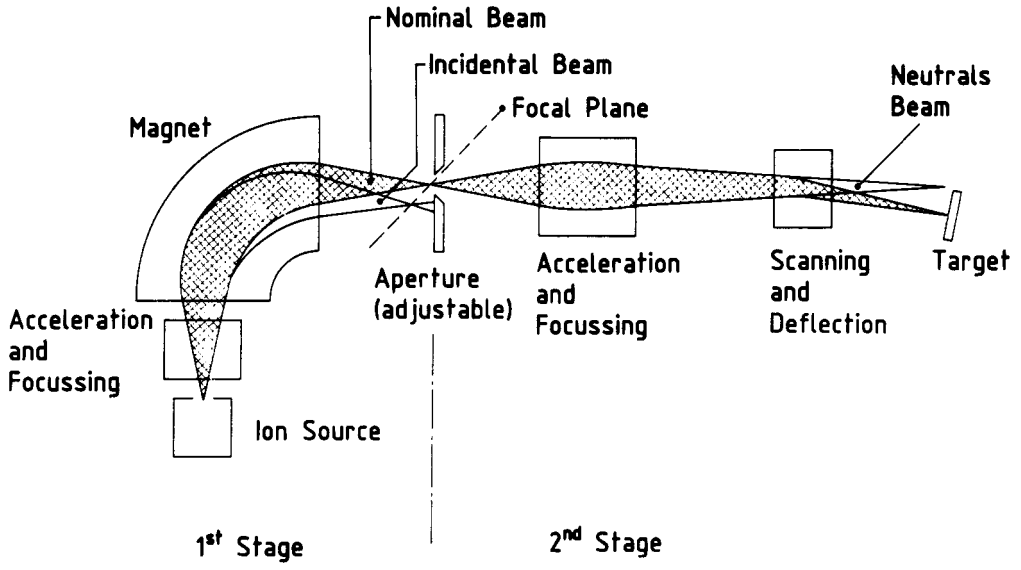

Fig. 2: Schematic lay-out of a two-stage ion implanter.

When materials scientists realized the potential of the process for the modification of materials (in particular for doping of semiconductor materials for electronic device manufacture), the design was changed to higher energy (several 10^5 eV) and higher ion current (several mA). In the new technological machines, called ion implanters, mass separation is sacrificed for higher ion current. The higher energy is attained by adding a second stage of acceleration beyond the focal plane of a scaled-down isotope separator.

An aperture at this focal plane is supposed to allow only the beam of the isotope of interest (i.e. the nominal constituent) to pass through. This cannot be achieved, though, at the low mass resolution ($M/\Delta M$ of about 150) of a high-current ion implanter. A neighbouring (M+1 or M−1) beam of an **incidental constituent** (Appendix 1) will overlap the beam of the nominal constituent to the extent that **cross contamination** in the nominal beam amounts to several percent from a neighbouring beam of equal intensity.

Among the many ion implanters currently in operation the technological implanters for semiconductor doping are most abundant. These are equipped with special **target stations** in which a number of wafers (up to 150 mm diameter) are successively brought into receiving position for the ion beam. The beam is scanned across the wafer until the desired dose density is attained. The 'integral over time of the electric current carried by the beam, divided by the charge per ion and by the area over which the beam is incident while being integrated' is used to derive the dose density.

In many target stations the beam current is monitored by overscanning into a detection device, called **faraday cup**. A properly designed faraday cup is supposed to collect all electric charges passed into the faraday cup as part of the beam, while disallowing any charge to pass out. Many so-called faraday cups do not comply with this requirement to the extent desirable for quantitative dosimetry. This is true in particular for another type of target station in which the wafer is placed at the bottom of a correspondingly wide-mouthed faraday cup rather than in a side-by-side configuration of target and faraday cup.

In both types of target station the wafer is stationary during scanning, and the beam is scanned in two directions, (called X and Y, where X is in the direction of mass number change in the mass spectrum). In an important modification of this concept the beam is scanned along the Y-axis only, while the wafer is moved (oscillated or rotated) along the X-axis; this is known as **hybrid scanning**.

The target (e.g. a single-crystal silicon wafer cut to face in the (111) crystallographic direction) is mounted at a tilt of 7° off normal so as to avoid **channeling** of the incident ions (in the (111) direction). A minimum distance of between 1 and 3 metres is kept between the scanner plates and the target for non-channeling conditions to be maintained at all points of incidence.

Interaction of ions with the residual gas (at typically 10^{-6} hPa) along the beam trajectory in the implanter leads to neutralization of a fraction of these ions. A **rule-of-thumb** (ref. 10) puts this fraction at 1% for a trajectory length of 1 m at a pressure of 1 hPa. This is the approximate pressure on the target station side of most implanters. Neutrals cannot follow an electrostatic or magnetic deflection of the beam. Hence, they are separated from the beam by beam deflection at the most foreward position possible; this is at the scanner plates. However, further neutralization occurs along the remainder of the trajectory. Therefore, the beam incident on the target may be accompanied by up to several percent of neutrals.

3. BEAM QUALITY

For definitions of the beam-related nomenclature Appendix 1 pertains. In routine ion implantation, in-situ ion dosimetry is used to obtain a value for the dose density of the implantant in the target material. In quantitative ion implantation in-situ ion dosimetry is relied upon for an accurate determination of the retained dose density of the implantant in the host material. Hence, in the latter case beam quality is of cardinal importance. This is dealt with in the following.

In the previous section, reference was made to **cross contamination** in the nominal beam, resulting from overlap of neighbouring incidental beams. The extent of overlapping can be derived from the value of the mass resolution $M/\Delta M$ of the implanter. The mass resolution (defined in section 2) is a measure of the relative width of the beam at given focussing conditions. This width is determined by aberrations due to beam shaping, by space charge effects in the beam, and by elastic small angle scattering of ions on residual gas along the beam trajectory.

An intensity profile of a nominal beam of $^{85}Kr^+$ ions measured at $M/\Delta M$ = 450 (ref. 19) is shown in Fig. 3. It allows the cross contamination to be estimated at the position of a neighbouring beam. On the (reasonable) assumption of an invariant beam shape for varying mass resolution one can derive also the values of cross contamination at other mass resolutions. For $M/\Delta M$ = 150, also shown in Fig. 3, these values are 0.7% of the peak intensity at the position of the nearest neighbour (here M = 86), and 0.4% at the position of the next-nearest neighbour (here M = 87). From the intensity profile of a $^{133}Cs^+$ beam (ref. 7) corresponding (and corroborative) values of 3% and 1% were derived. The intensity profile in Fig. 3 has been determined on an implant of the radioactive ^{85}Kr from a stationary beam. Therefore, the profile represents the sum of $^{85}Kr^+$ ions and ^{85}Kr neutrals. As pointed out before (ref. 7), the proportion of neutrals is not constant across the profile, but is larger in the wings. In fact, for mass resolution 450 the cross contamination at the neighbouring mass position consists predominantly of neutrals. The implication is that for mass resolution 450 the cross contamination by *ions* is actually less than half the figures quoted. For mass resolution 150 the cross contamination is predominantly ionic. For isotopic cross contamination (where charge state is not of concern) the figures remain as quoted.

It is concluded that actual percentages of cross contamination in a nominal beam can be several times higher than these values if the incidental beam is of higher intensity than the nominal beam, and if more than the full width at half maximum of the intensity profile of the nominal beam is allowed to pass through the aperture at the focal plane (of the first stage of the implanter). In technological ion implanters of low mass resolution, cross contamination can be reduced (though not eliminated) by avoidance of strong neighbouring beams and use of a narrow aperture at the focal plane of the first stage.

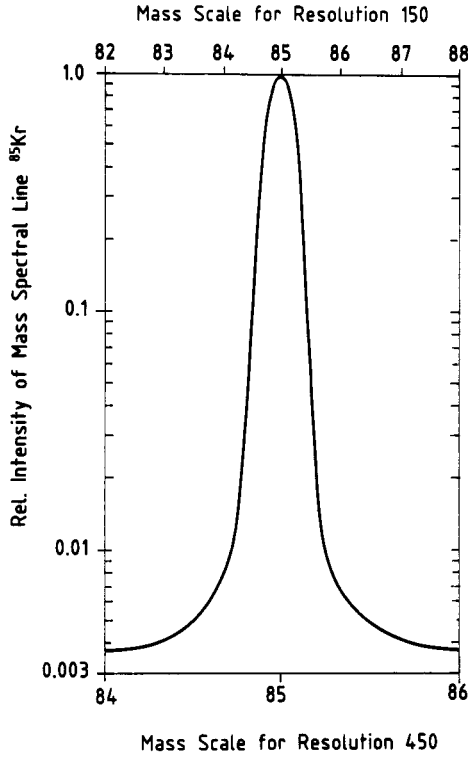

Fig. 3: Intensity profile of a (nominal) $^{85}Kr^{+}$ beam focussed to a mass resolution of $M/\Delta M$ = 450 (lower abscissa scale; the upper abscissa scale pertains to a mass resolution of 150). ^{85}Kr neutrals are included in the profile.

The very low levels of cross contamination attainable in an optimally tuned electromagnetic isotope separator have been documented by Uhler (ref. 20) and Uhler and Rossi (ref. 21) (who show intensity profiles of ^{85}Kr beams of different charge states in dependence on the residual gas pressure).

While it can be argued that a cross contaminant should be acceptable if it is an isotope of the implantant and if the intended application of the reference material is not isotope-specific, such acceptance is discouraged even then because (1) the cross-contaminating ions are deflected ions and constitute an ion optical aberation, and (2) for a number of technological ion implanters cross contaminating ions have been reported (ref. 22) to be energy-deficient.

Also mentioned in section 2 was the presence of **neutrals** of the implantant, both before and after beam deflection at the scanner plates. It was pointed out that even after this separation the nominal beam can be accompanied by a percentage value of neutrals. The rule-of-thumb mentioned earlier, according to which the percentage is about equal to the product of the beam length in metres and the residual gas pressure in hectopascal, allows the acceptable pressure to be estimated for a given beam length.

There are additional constituents in the beam which for purposes of quantitative ion implantation must be considered as undesirable impurities. These are: Incidental constituents having the same mass-to-charge ratio as the implantant (here called 'isobaric contaminants'), Aston bands, and drift electrons.

An **isobaric contaminant** can be either an isotope of a neighbouring chemical element, or, more likely, a cluster particle. Once part of the nominal beam, such a contaminant behaves in exactly the same way as the implantant. Isobaric contamination can be avoided only by a judicious choice of those materials which may, by their presence in the ion source (e.g. as wall material), participate in the total ion beam.

Aston bands originate from muliply-charged ions undergoing a charge change, and/or from cluster ions undergoing a mass change, both in interaction with residual gas in the pre-magnet region of the first stage of an ion implanter.

The contamination appears as a broad mass band at the focal plane of the first stage. Again, the intensity is proportional to the residual gas pressure (in the pre-magnet region). The low probability of multiple ionization in standard ion sources and the wide mass spread of the bands cause this type of contamination to be of lesser importance. Still, it may be an important part of the general background.

The general **background** in the mass spectrum consists of contributions from all constituents in the total beam. Most ions in the background have undergone angular deflection in interaction with residual gas or with hardware. The background can be determined in a blind run in which the nominal constituent (and its isotopes) are absent. The background inclusive of any remaining contaminant mass spectrum (due, for instance, to ion source 'memory') can then be measured. A pre-condition is that during the blind run, ion source conditions must be identical to the actual run. This can be guaranteed only if the chemical interaction between the nominal constituent and other materials in the ion source is at an insignificant level. Much depends on the wall material of the ion source; reactor grade graphite is preferable over stainless steel.

Secondary electrons are generated where beam meets hardware. Some of these electrons are captured by the space charge region of the ion beam and, thereby, become **drift electrons**. While these electrons fulfill an important function in beam focussing, they are detrimental to the ion current measurement. Hence, they must be kept out of the faraday cup by a negative barrier field at the cup entrance.

A more detailed exposition of contamination in ion beams can be found in ref. 10 as well as in earlier studies by Freeman et al. (ref. 23), Uhler (ref. 20), and Uhler and Rossi (ref. 21).

In summary, ion dosimetry of the nominal constituent will be in error by the percentages of cross contamination, of neutrals, of isobars and of background. While isobars are relatively easy to avoid and background can be dealt with through an intense nominal beam, cross contamination and neutrals are everpresent problems in most ion implanters. The fact that the errors due to cross contamination and to neutrals cancel each other in part is no consolation, because implantation conditions appear to be better than they actually are. In fact, if agreement is found between post-implantation measurement of the retained dose density and in-situ dosimetry in a technological implanter such agreement is bound to be due to a fortuitous combination of errors. Lowering the residual gas pressure (and/or shortening the distance) between scanner plates and target are effective measures against neutrals. The problem of cross contamination has to be investigated anew for each case. Cross contamination can be reduced by ensuring best possible focus and by sacrificing intensity of the nominal beam at the first-stage aperture for a better implantant-to-contaminants ratio.

Considering all of the above, it must be concluded that ion implanters of the high-current technological type described in section 2 are rather unsuitable for quantitative ion implantation. Only implanters with a mass resolution ≥ 500 offer good enough prospects for elimination of the problems mentioned above. In consequence, only the latter type of implanter (i.e. the research type implanter) is suitable for the preparation and part-certification of primary reference materials (cf. section 7). Secondary and working reference materials (cf. section 7), on the other hand, can be prepared in technological implanters on provision that isotopic cross contamination be rendered insignificant. For secondary and working reference materials, in-situ ion dosimetry would not have to be relied upon for certification, and the dose densities claimed by suppliers would be used for guidance only.

4. BEAM INCIDENCE ON A TARGET AND RETENTION OF AN IMPLANTANT

Once the quality of a nominal beam has been ensured, the retention of the implantant has to be considered. In the following, the derivation of the retained dose density from in-situ dosimetry is dealt with in section 4.1, and problems in sections 4.2 and 4.3. Dose density limits are derived in section 4.4, and concentration levels in section 4.5.

4.1 Dose density

It is common practice to calculate the dose density from the integral over time of the beam current and the geometrical area over which the beam is incident while being integrated. As pointed out in section 2, this integration proceeds either on-target (if the target is inside the faraday cup) or side-by-side with the target (in a separate faraday cup). In both cases it is the size of the aperture through which the beam is admitted into the faraday cup which enters into the calculation of dose density. This practice is believed to be a major source of error for dose density values quoted by suppliers. In the on-target case, the assumption is that a one-to-one correspondence exists between cup-aperture size and implanted area. This is correct only for a strictly parallel beam, for invariant angles of incidence and for a uniform scanning pattern. The latter two are also preconditions in the side-by-side case, and, furthermore, the cup-aperture size should not be affected by sputter erosion. Normally, these conditions are not met. A type of scanning in which these conditions are met is the particular mode of hybrid scanning shown in Fig. 4*a*. This mode, which is uncommon in technological implanters, is recommended for quantitative ion implantation. An alternative X-Y scanning mode, which can also be considered for quantitative ion implantation, is shown in Fig. 4*b*, provided one can ensure that the angle of incidence and the scanning pattern remain invariant across the scanned area.

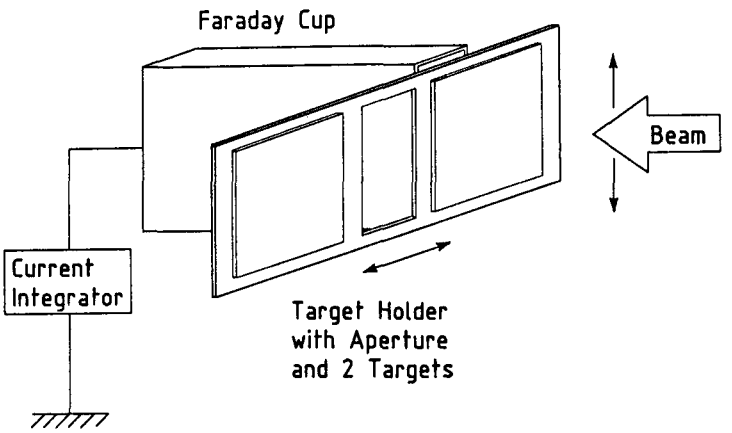

Fig. 4a: The hybrid mode of beam scanning recommended for quantitative ion implantation (see text). The design of the faraday cup (shown schematically) must meet stringent requirements discussed elsewhere (e.g. ref. 12).

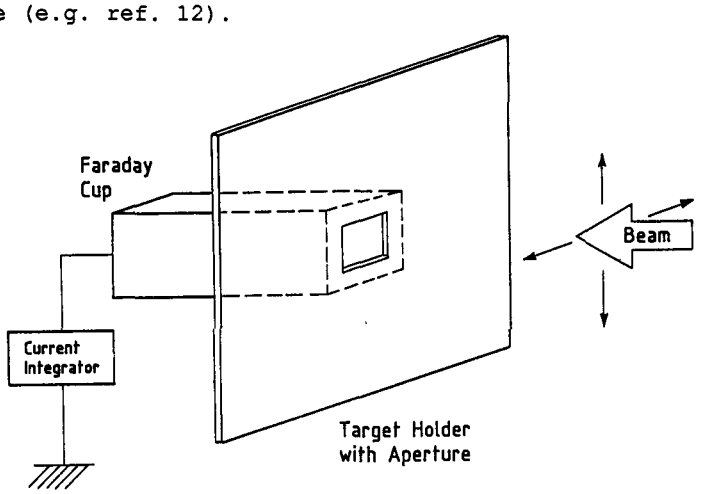

Fig. 4b: An X-Y scanning mode which can also be considered for quantitative ion implantation on condition that the angle of incidence and the scanning pattern remain invariant across the scanned area.

The uniformity of beam scanning needs to be confirmed for each implantation undertaken for the preparation of reference materials. In the investigations published, best non-uniformities reported for technological implanters are of the order of 1% for a 50mm scan; larger values are not infrequent. These non-uniformities were measured with lateral resolution in the millimeter range. This author is not aware of investigations of dose densities at higher spacial resolution. Much will depend on the relationship between beam width and line spacing in a scanning pattern, on the number of complete frames, on the linearity and smoothness of the scanning voltages, and, again, the constancy of the angle of incidence. Quantitative ion implantation calls for less focus, more frames, and an invariant angle of incidence.

The dose density of implantant present in the target material at the end of the process of implantation - i.e. the retained dose density - is the quantity of interest. Ion dosimetry of a nominal beam of 100% purity provides a value of the received dose density. This quantity splits into two fractions, an implanted dose density and a non-implanted dose density. Implantant atoms belonging to the former fraction are trapped inside the target; those belonging to the latter fraction are re-emitted before being trapped. The implanted dose density suffers losses due to sputtering of the target surface (insignificant at first, substantial in the end). The remaining implantant constitutes the retained dose density. Fig. 5 pertains.

In Table 1 are displayed all charge and particle densities which play a role in quantitative ion implantation. The symbols in the table are used below to show the relationships between these densities by simple formulae. In terms of the symbols used in Table 1 the situation in quantitative ion implantation can be expressed as follows:

The quantity q is what is measured, and d_a^{ret} is the quantity to be derived therefrom. Each of these can in turn be expressed as

$$q = q_{ia} + q_{ic} + q_e \qquad (1)$$

$$d_a^{ret} = d_a - (d_a^{nim} + d_a^{sp})$$

$$= d_{ia} + d_{na} - (d_a^{nim} + d_a^{sp}) \qquad (2)$$

The only direct link between electric charge density and particle dose density exists between q_{ia} and d_{ia}, viz.

$$d_{ia} = q_{ia} / z \qquad (3)$$

where z denotes the charge number of the ions of analyte. The use of a well-designed faraday cup is assumed here.

In quantitative ion implantation, conditions are chosen such that minimization is achieved for q_{ic} and q_e in eq. 1 as well as for d_{na}, d_a^{nim} and d_a^{sp} in eq. 2 (see also Fig. 5). How q_{ic}, q_e and d_{na} are dealt with has been explained in section 3. The remaining quantities are treated in the following.

4.2 Backscattering

Hosts for reference materials are usually thick, i.e. they are not transparent to the energetic implantant. Still, implantant atoms can leave the host by being backscattered before having slowed down sufficiently to be trapped. These atoms constitute the non-implanted dose density, denoted by d_a^{nim}.

Backscattering must be assumed to be non-negligible if the mass number (A_1) of the implantant is lower than that of the major constituent of the host (A_2). In many such cases, percentage values of non-implanted ions/atoms can reach 2-digit figures. The percentage value depends on the mass number ratio A_1/A_2, the ion energy, and the angle of incidence; it increases for lower mass ratio, lower ion energy, and more oblique angle of incidence.

Table 1. Symbols for particle and charge densities (cm^{-2})

	incident on the surface					passing into the solid		
	nominal	incidental			total	non-impl.	implanted	
		neutrals	ions	electrons			sputt.	ret.
heavy particles	d_{nom} = d_{ia}	d_{inc}: d_{na}	d_{ic}		d			
analyte only	d_{ia}	d_{na}	-		d_a	d_a^{nim}	d_a^{im}: d_a^{sp}	d_a^{ret}
electric charge	q_{ia}	-	q_{ic}	q_e	q			

Subscripts: nom = nominal; inc = incidental; a = analyte; ia = ions of analyte; na = neutrals of analyte; ic = ions of contaminants; e = electrons

Superscripts: nim = non-implanted; im = implanted; sp = sputtered; ret = retained

Note: The definitions associated with these symbols are to be found in Appendix 1 (Terminology).

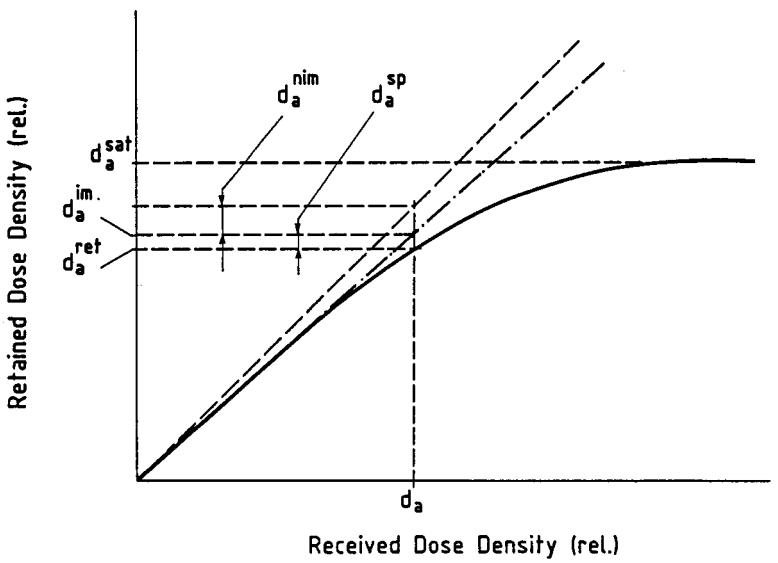

Fig. 5: The collection curve of ion implantation (see sections 4.1 and 4.4 for details).

Eckstein and Biersack (ref. 24) have published an extensive theoretical study of backscattering based on the well-known TRIM code. Although some measurements are available for comparison of these results with experiment, the present coverage is not considered sufficient to allow the theoretical predictions to be used in quantitative ion implantation. Important general conclusions can be drawn, though, from the results of the study. For this purpose, excerpts are shown in Tables 2 and 3.

Table 2. Backscattering of implantant for normal and near-normal incidence (α = angle of incidence)

System	A_1 / A_2	Energy (keV)	Backscattered fraction (%)	
			$\alpha = 0^o$	$\alpha = 15^o$
^{42}K - Ag	0.38	30	8.2	8.8
^{24}Na - Ag	0.22	30	12.1	13.5
^{42}K - Au	0.21	30	17.9	19.4
^{24}Na - Au	0.12	30	22.9	23.3
do.	do.	3	35	
do.	do.	300	10	

Table 3. Minimum energy (E_{min}) for backscattering <1% and <3% at normal incidence

System	A_1 / A_2	E_{min} (keV) for backscattering	
		<1%	**<3%**
^{12}C - C	1	0.6	0.02
^{103}Rh - Rh	1	60	2
^{209}Bi - Bi	1	250	8
^{42}K - Ag	0.38	650	250
^{24}Na - Ag	0.22	600	200
^{42}K - Au	0.21	2000	700
^{24}Na - Au	0.12	1600	650

In summary: For $A_1 > A_2$, energies >100 keV (say), and at normal incidence, the backscattered fraction remains well below 1% in most cases. It can exceed 1% if both A_1 and A_2 are large; but even then, the fraction does not exceed 2% for $A_1 = A_2$. For $A_1 < A_2$, energies have to be raised to beyond those attainable in most ion implanters if the backscattered fraction is to be kept below 1%. The backscattered fraction is not very sensitive to a several degrees departure from normal incidence. Thus, in general, values of $d_a^{nim} \leq 0.01\ d_a$ can be obtained by restricting quantitative ion implantation to implantant/target systems for which $A_1 > A_2$, and to near-normal incidence at an appropriately high energy. These provisos are part of the boundary conditions for quantitative ion implantation

4.3 Sputtering

Sputtering of the target surface sets in with implantation of the first ion. The thickness of the target material sputtered away is roughly proportional to the received dose density. The departure from a strict proportionality is caused by the materials-modifying effect of the implantation and sputtering processes. The relationship between material removed and received dose is expressed in the **sputtering yield**, which gives the average number of atoms (and ions) sputtered for each incident ion. The sputtering yield changes with implantant/target system, ion energy and angle of incidence. It is different for an impurity-covered (e.g. oxide) surface. Experimental values of sputtering yield normally pertain to prolonged sputtering, i.e. to a fully modified target. Transitional changes of sputtering yield are lumped together with the sputtering yield of the modified target. The values published, are usually underspecified. In contrast, theoretically derived values pertain to the idealized situation of a virgin target material, flat-surfaced and free of surface impurities. While theoretical values tend to be unrealistic also because of other simplifying assumptions, theory allows dependences to be recognized and experimental data to be systematized. The sputtering yields displayed in Figs 6 *a* to *e* were derived in this way, i.e. a large number of experimental values were systematized (refs. 25, 26, 15) by use of the theory of Sigmund (ref. 27). The figures (first published in ref. 15) show the sputtering yield $S^{(1eV)}$ as a function of ion energy, with the atom numbers Z_1 and Z_2 of implantant and target respectively as parameters. The sputtering yields are for normal incidence and have been normalized for a surface binding energy U of 1 eV per sputtered atom. Hence, the actual sputtering yield is obtained therefrom as $S = S^{(1eV)}/U$. The values of U used in the derivation of $S^{(1eV)}$ are listed in Table 4; they were selected from a tabulation of sublimation enthalpies (ref. 28).

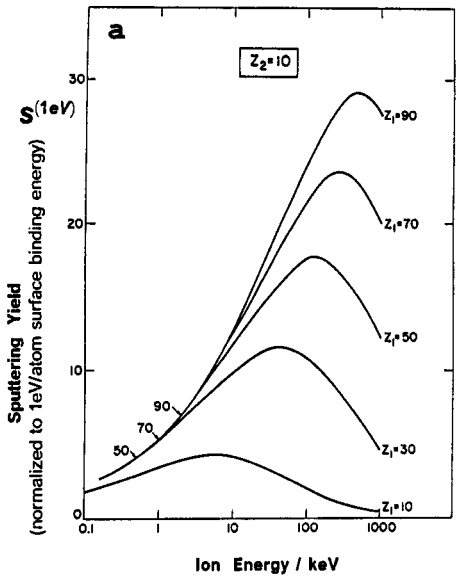

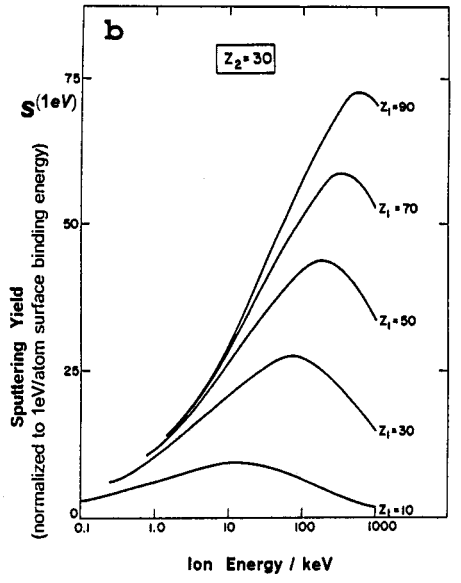

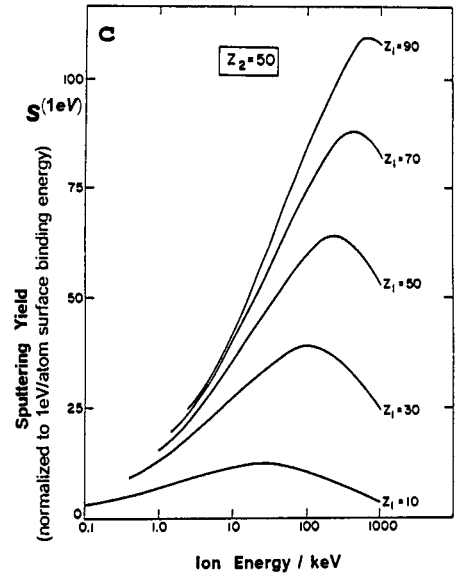

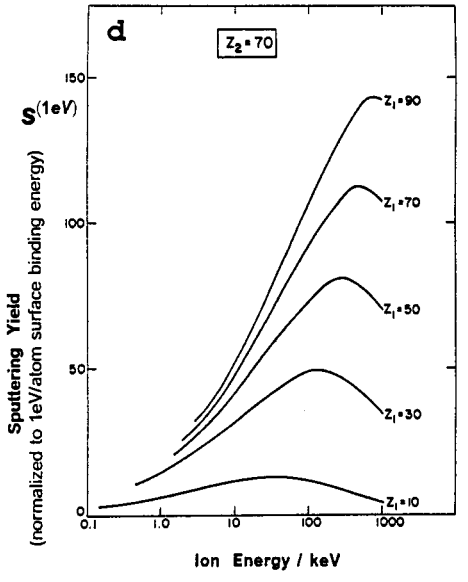

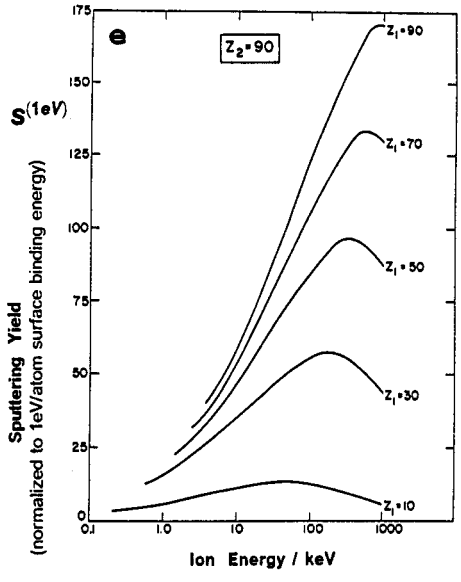

Figs. 6 a-e: The normalized sputtering yield $S^{(1eV)}$ (i.e. for a surface binding energy of 1 eV) as a function of ion energy, with the atom numbers Z_1 and Z_2 of implantant and target resp. as parameters.

Table 4. Surface binding energies (U, eV/atom) of solid chemical elements (in alphabetical order)

Ag:2.95	Al:3.42	As:3.13	Au:3.82	B :5.92	Ba:1.89	Be:3.36	Bi:2.17
C :7.43	Ca:1.85	Cd:1.16	Ce:4.38	Co:4.44	Cr:4.12	Cs:0.79	Cu:3.49
Dy:3.01	Er:3.29	Eu:1.82	Fe:4.31	Ga:2.82	Gd:4.12	Ge:3.88	Hf:6.42
Ho:3.12	In:2.52	Ir:6.94	K :0.93	La:4.47	Li:1.65	Lu:4.44	Mg:1.52
Mn:2.94	Mo:6.83	Na:1.11	Nb:7.48	Nd:3.40	Ni:4.46	Os:8.18	P :3.46
Pb:2.02	Pd:3.91	Pr:3.69	Pt:5.86	Pu:3.65	Rb:0.84	Re:8.04	Rh:5.74
Ru:6.76	S :2.88	Sb:2.74	Sc:3.92	Se:2.32	Si:4.73	Sm:2.14	Sn:3.12
Sr:1.88?	Ta:8.11	Tb:4.03	Te:2.04	Th:5.97	Ti:4.87	Tl:1.88	Tm:2.41
U :5.43	V :5.33	W :8.81	Y :4.41	Yb:1.58	Zn:1.35	Zr:6.31	

4.4 Collection curve of ion implantation, and limiting dose density

Fig. 5 pertains. The sputtered dose density d_a^{sp} consists of that fraction of the implanted dose density which is part of the sputtered-away thickness of target surface. This fraction increases with sputtered-away thickness, and, hence, with received dose density. In consequence, the rate at which the implantant is re-sputtered increases towards the rate at which the implantant is received. Eventually, the two rates become equal and the retained dose density levels off at a constant value, known as saturation value (d_a^{sat} in Fig. 5). The saturation value is first reached at a sputtered-away thickness of roughly twice the mean depth of ion penetration in the target. The transition from the initial proportionality between received and retained dose densities to the saturation value is schematically displayed in Fig. 5; the relationship is known as **collection curve**. Also, the relationship expressed in eq. 2 is displayed.

The conditions for quantitative ion implantation are summarized again with reference to Fig. 5:

The value of d_a^{ret} is derived from that for d_a (eq. 2), which in turn is derived from that for q_{ia} (eq. 3). The latter is derived from a measurement of q (eq. 1) on condition that q_{ic} and q_e are negligible.

In order to derive d_a^{ret} from d_a (eq. 2), each of the quantities d_a^{nim} and d_a^{sp} must either be known to good accuracy or rendered negligible. For reasons explained above, it is recommended that d_a^{nim} be rendered negligible (i.e. <1% of d_a) by restricting quantitative ion implantation to cases where $A_1 > A_2$, and to near-normal incidence at an appropriately high energy. The value of d_a^{sp} can be calculated from the depth distribution of the implantant in the target and from the sputtering yield. Neither quantity is known sufficiently well for an accurate prediction of d_a^{sp}. Hence, the likelihood of a large error on the calculated value of d_a^{sp} must be accommodated. Therefore, it is recommended that quantitative ion implantation be restricted to dose densities d_a below a limiting value d_a^l at which $d_a^{sp} = 0.01\ d_a$, or equivalently $d_a^{ret} = 0.99\ d_a$ (i.e. 99% retention). In other words, quantitative ion implantation is restricted to the initial straight-line and qasi-straight-line part of the collection curve in Fig. 5.

Limiting dose densities d_a^l were calculated (refs. 29, 15) for $d_a^{sp} = 0.01\ d_a$ (i.e. 99% retention) as well as for $d_a^{sp} = 0.05\ d_a$ (i.e. 95% retention). These were calculated for two different depth penetration probability densities, viz. Gauss and Cauchy. The choice of these two functions is in conformity with the argument (section 5) that implantant profiles should be representable by split Student-t functions. Student-t functions comprise a family of functions,

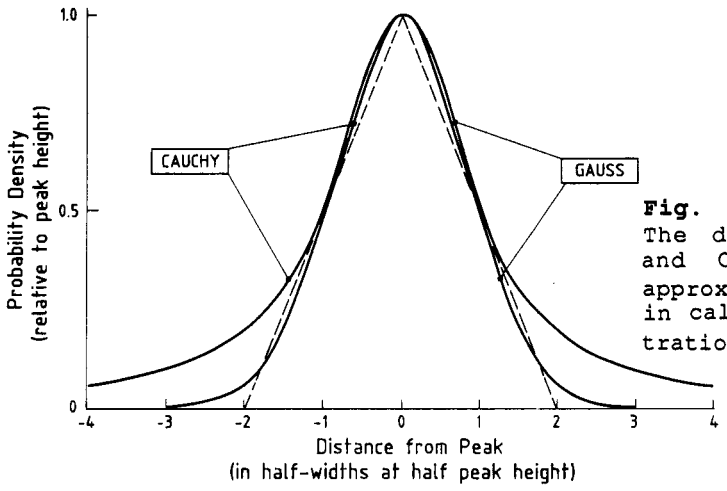

Fig. 7:
The distribution functions Gauss and Cauchy, and a triangular approximation (broken lines) used in calculation of the peak concentrations in Table 5a.

distinguishable by an integer shape parameter, known as the degrees of freedom (ν), with the Cauchy function (ν = 1) at the one extreme, and the Gauss function (ν = infinity) at the other extreme. Both functions are shown in Fig. 7, normalized to the same peak height and to the same half-width at half maximum. Split Student-t functions are made up of two half-functions with different shape parameters. Since the function pair Gauss and Cauchy can be considered as bracketing functions to all possible split Student-t functions, they can be used to calculate highest and lowest limiting dose densities. The most probable limiting dose density would be somewhere between these two, while the 'safest' limiting dose density would coincide with that for a Cauchy function.

Values of $d_a^{1(1eV)}$, calculated for a depth penetration probability density of a Cauchy form and another of a Gauss form, both for 99% and for 95% retention, for $A_1 > A_2$, are shown in Figs 8 *a* to *d* (first published in ref. 15). The values are shown as a function of the atomic number Z_1 of the implantant, with the ion energy and the atomic number Z_2 of the target as parameters. The sputtering yields used were those shown in Figs 6 *a* to *e*. As in the case of the sputtering yields $S^{(1eV)}$, the values of $d_a^{1(1eV)}$ are for normal incidence and have been normalized to a surface binding energy U of 1 eV per sputtered atom. Hence, the actual limiting dose density is obtained therefrom as $d_a^1 = U.d_a^{1(1eV)}$.

The values of $d_a^{1(1eV)}$ are seen to depend very much on ion energy as well as on the atomic numbers Z_1 and Z_2 of implantant and target respectively. The high values of $d_a^{1(1eV)}$ for a low-Z implantant and a low-Z target at high ion energies drop by almost three orders of magnitude if the energy is lowered from 300 keV to 10 keV. They drop by four orders of magnitude if Z_1 and Z_2 rise from 10 to 80 at a constant energy of 300 keV, and by two orders of magnitude at an energy of 10 keV. The type of depth distribution (Gauss or Cauchy) is of lesser importance; it is of more significance at 99% retention than at 95% retention.

For a Gauss distribution and 99% retention, the values of $d_a^{1(1eV)}$ range from about 2×10^{18} cm^{-2} for 300 keV ions of $Z_1 = 10$ on a target of $Z_2 = 10$ to about 3×10^{13} cm^{-2} for 10 keV ions of $Z_1 = 80$ on a target of $Z_2 = 80$. Corresponding values of $d_a^{1(1eV)}$ are a factor of 2 lower for a Cauchy distribution. Corresponding values of $d_a^{1(1eV)}$ are a factor of 3 higher for 95% retention. Since most actual depth profiles are closer to the Gauss form than to the Cauchy form, the actual values of $d_a^{1(1eV)}$ can be expected to be biased towards those for the former.

In general, it may be said that in a broad middle range and the high range of atomic numbers the values of $d_a^{1(1eV)}$ range from a few 10^{14} to a few 10^{16} cm^{-2} for ion energies between 10 and 300 keV. Hence, over the same ranges of atomic numbers and energies, values of d_a^1 range from about 10^{15} to 10^{17}cm^{-2}. As an example, in the (worst) case of a Cauchy distribution, a limiting dose density

d_a^1 of about 1 x 10^{14} cm^{-2} is predicted for 99% retention of normally incident 10 keV Tl-ions (Z_1 = 81) into Au (Z_2 = 79, U = 3.8 eV/atom).

As far as is known, no systematic attempt has been made for an experimental confirmation of theoretical retention values. It would have to be based on finding the closest possible agreement between the dose density d_a in eq. 2, as derived from an in-situ measurement (performed under conditions of quantitative ion implantation) of the on-surface net-electric-charge density q in eq. 1, on the one hand, and the retained dose density d_a^{ret}, as determined in a post-implantation measurement of suitable accuracy, on the other. Very few of these

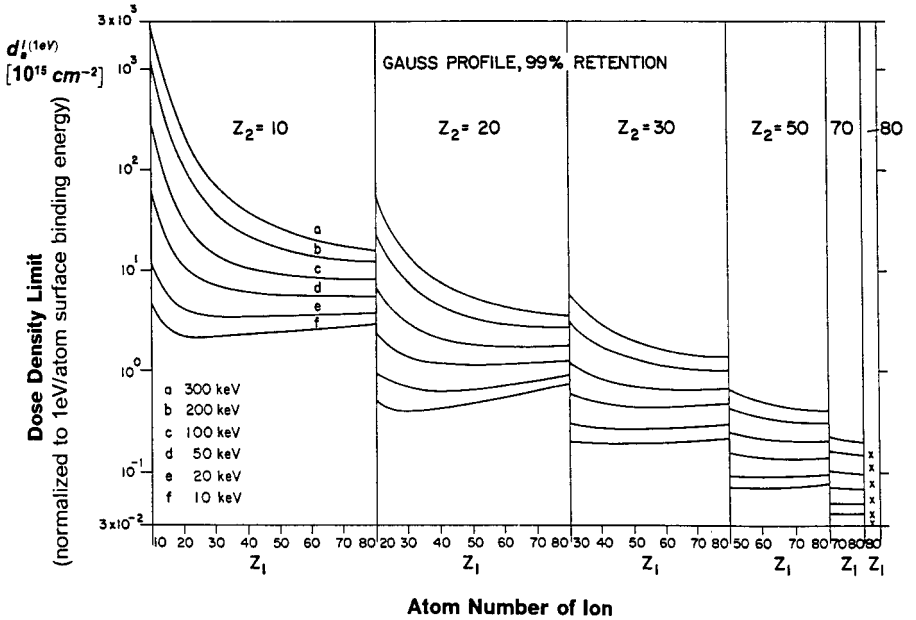

Fig. 8a: Theoretical limiting dose densities $d_a^{l(1eV)}$, normalized to 1 eV surface binding energy, for an implantant retention of 99% given that the depth penetration probabilty density is represented by a Gauss distribution (see Fig. 7).

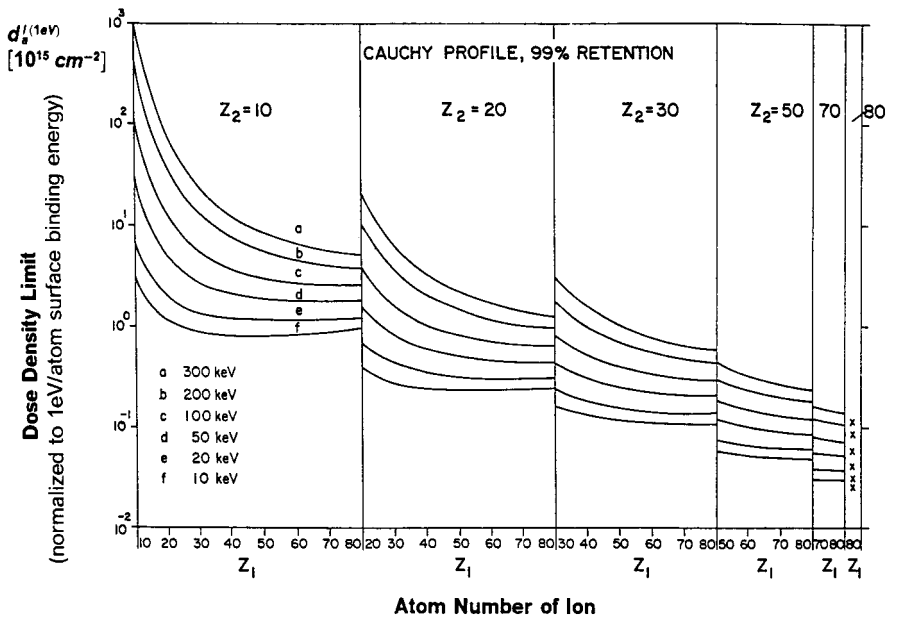

Fig. 8b: As for Fig. 8a, but for a Cauchy (rather than Gauss) distribution.

measurements have been reported, for the obvious reason that retention measurements of the required accuracy are extremely difficult to perform. The closest agreement between d_a and d_a^{ret} reported to date for conditions of quantitative ion implantation is that for 40 keV $^{85}Kr^+$ implanted into polycrystalline aluminium when the ratio d_a/d_a^{ret} = 1.0057 ± 0.007(standard deviation) was obtained for a series of 7 implants at 7 different dose densities below the theoretically predicted limiting dose density (ref. 4).

For a decision on whether the (theoretical) limiting dose densities of Figs 8 *a* to *d* are indeed (firstly) safe values, and (secondly) realistic values, reliable actual collection curves have to be available. Although some collection curves are found in the literature, these are usually plotted to non-absolute scales. These curves allow the ratio d_a^{sp} / (d_a^{ret} + d_a^{sp}) to be derived, as a function of

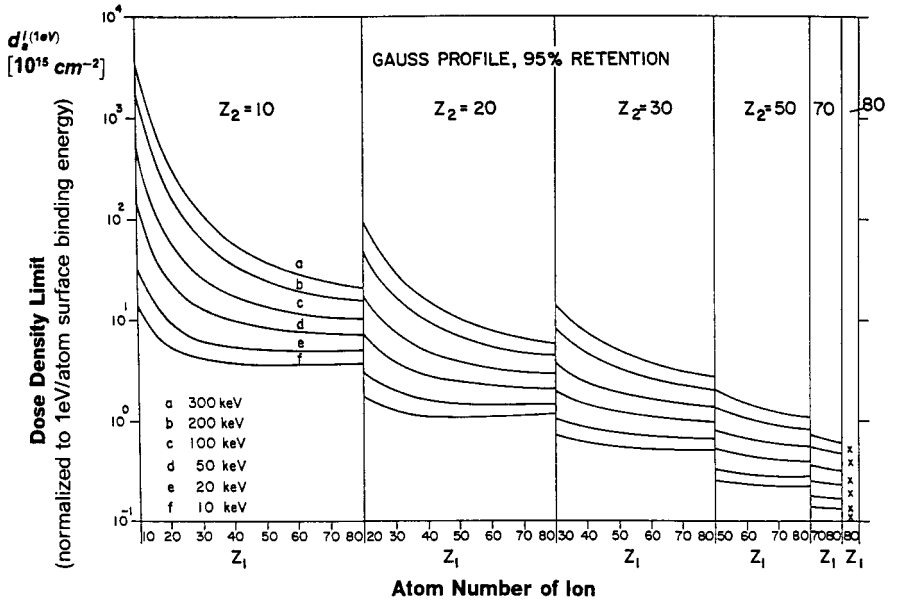

Fig. 8c: As for Fig. 8a, but for an implantant retention of 95% (rather than 99%).

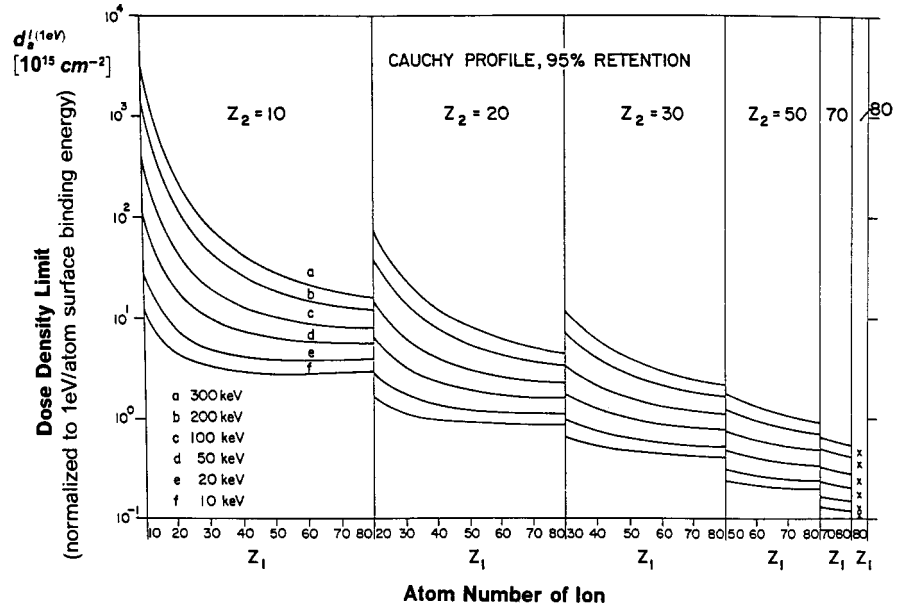

Fig. 8d: As for Fig. 8a, but for an implantant retention of 95% and for a Cauchy distribution.

what is usually called the incident fluence or dose (in reality the ratio q/z, where z denotes the charge number of the ions of analyte) of unknown accuracy. Approximate values of the limiting dose density can be derived therefrom, on the assumption of insignificant backscattering, and using the criterion that the collection curve must initially be a straight line. These results suggest that for the few systems tested the theoretical values of d_a^1 in Figs 8 *a* to *d* can be regarded as useful figures of guidance. They are safe (i.e. they are on the low side of the experimental value, sometimes by a factor of 2 or 3), though not always realistic. This conservative behaviour can be linked to differences between the actual conditions on the surface and the model (not discussed here). It must be emphasized that these differences may not always lead to a conservative behaviour in other systems.

4.5 Implantant concentration

The depth profile of concentration of implantant corresponding to a given dose density d_a is the ultimate information to be certified in an ion-implanted reference material. This information is not available at present. The problems are discussed in section 5. One must do with approximations instead. Two key values are the implantant concentration at the distribution peak (in the following called peak concentration) and the concentration at the surface.

4.5.1 *Peak concentration*

For an estimate of the concentration at the distribution peak the following approximation is used:

The depth distribution is treated as a symmetrical triangular distribution as shown in Fig. 7. The peak depth and the half-width-at-half-maximum are assumed to be given by the (theoretically derived) quantities known as the **projected range** R_p and the **projected range straggling** ΔR_p (i.e. the standard deviation of the projected range), published in a number of tables. Then, the peak concentration c_{pk} at a dose density d_a is given by

$$c_{pk} = 0.083 \times 10^{-15} \, d_a \, A_2 \, / \, \Delta R_p \quad \text{at.\%} \qquad (4)$$

if ΔR_p is given in mg.cm^{-2} and d_a in atoms.cm^{-2}. As before, A_2 is the mass number of the target material.

The peak concentration c_{pk}^1 at the limiting dose density d_a^1 is derived from eq. 4 if d_a^1 is substituted for d_a, where d_a^1 (atoms.cm^{-2}) is given by $U.d_a^{1(1eV)}$, and $d_a^{1(1eV)}$ is taken from Figs 8 *a* to *d*.

The values of c_{pk} calculated from eq. 4 are too high by 5% if the depth distribution is of Gauss form; they are too high by a factor of 1.5 if the depth distribution is of Cauchy form. For the majority of actual distributions these values of c_{pk} are expected to be too high by between 10 and 20%.

Selected values of c_{pk}, calculated from eq. 4 for a dose density $d_a = 10^{15}$ cm^{-2}, are listed in Table 5*a*, together with the corresponding values of R_p (mg.cm^{-2}) and ratios R_p / ΔR_p (excerpted from ref. 29). These values are tabulated as a function of atomic numbers Z_1 (implantant) and Z_2 (target), as well as of ion energy E; other values of c_{pk} (Z_1, Z_2, E) can be derived by interpolation. The calculation has been simplified by adopting fixed ratios of A/Z as shown in Table 5*b*.

The values of c_{pk} listed in Table 5*a* scale with the dose density d_a. It is concluded that peak concentrations often reach two-digit percentages for the high limiting dose densities of the low-Z target materials. It should be noted that (1) at the two-digit percentage level corrections are called for to the model of quantitative ion implantation (which in turn affect the values of d_a^1), and (2) reference materials cease to be classifiable as dilute solid solutions already at 3 at.% implantant concentration (see section 6). Hence, Table 5*a* has an important function in the decision on the maximum permissible dose density for a reference material.

Table 5a. Approximate peak concentrations c_{pk} for a dose density $d_a = 10^{15}$ cm^{-2}, and associated values of the location and scale parameters R_p and ΔR_p of the depth distribution.

E(keV)		10	30	100	300	10	30	100	300	10	30	100	300
Z_1	Z_2	R_p (μg.cm^{-2})				R_p / ΔR_p				c_{pk} (at.%)			
10	10	4.2	12	43	126	2.0	2.4	3.4	5.7	.83	.35	.14	.08
20		2.6	6.4	20	63	2.3	2.5	2.8	3.6	1.5	.68	.24	.10
30		2.2	5.0	14	41	2.7	2.8	2.9	3.3	2.1	.98	.36	.14
50		1.9	4.2	10	27	3.4	3.4	3.6	3.7	3.1	1.4	.63	.24
80		1.9	4.0	9.2	21	4.3	4.3	4.5	4.5	4.0	1.9	.86	.37
20	20	3.6	8.8	26	81	1.8	2.0	2.3	2.9	1.8	.83	.32	.13
30		2.9	6.6	18	52	2.0	2.2	2.3	2.6	2.5	1.2	.47	.18
50		2.5	5.3	13	33	2.6	2.6	2.7	2.8	3.8	1.8	.76	.31
80		2.3	4.7	11	25	3.1	3.1	3.3	3.3	4.9	2.4	1.1	.48
30	30	3.5	8.1	22	61	1.8	1.9	2.1	2.4	2.9	1.3	.53	.22
50		2.9	6.2	15	38	2.2	2.3	2.3	2.4	4.2	2.1	.86	.35
80		2.6	5.4	12	28	2.6	2.7	2.7	2.8	5.6	2.8	1.3	.56
50	50	4.0	8.3	20	49	1.9	1.9	1.9	2.1	4.5	2.3	.93	.42
80		3.4	6.9	16	36	2.2	2.2	2.2	2.3	6.4	3.1	1.4	.63
80	80	4.5	9.2	21	46	1.8	1.8	1.9	1.9	6.6	1.9	.89	.63

Table 5b. Mass numbers (A) associated with atom numbers (Z) in Table 5a.

Z_1 and Z_2	10	20	30	40	50	60	70	80
A_1 and A_2	21	44	67	92	118	144	171	199

4.5.2 *Surface concentration*

The surface concentration of implantant is another quantity of interest. Theoretical values can be obtained from the model of quantitative ion implantation (ref. 9). Approximate values of the surface concentration c_s can be derived from the combined use of Fig. 7 and Table 5a: If the ratio R_p / ΔR_p in Table 5a is equated to the ascissa values (in half-width at half maximum, *HWHM*) in Fig. 7, then the ordinate values in Fig. 7 will provide the fraction of the peak concentration c_{pk} to be expected at the surface. For example, for *HWHM* = R_p / ΔR_p = 2.0 , the surface concentration c_s equals 0.06 c_{pk} for a Gauss form of the depth distribution, and 0.19 c_{pk} for a Cauchy form. Hence, for (Z_1, Z_2) = (10, 10) at 10 keV and $d_a = 10^{15}$ cm^{-2} (Table 5a), c_s = 0.05 at.% for a Gauss form, and c_s = 0.10 at.% for a Cauchy form (the value of c_{pk} has been corrected for the Cauchy form, see discussion of Table 5a). Surface concentrations for other Student-t forms of the depth distribution can be obtained by the use of Fig. 9 instead of Fig. 7.

The author is not aware of any experiment in which these predicted values of c_s feature as reference values. It is conceivable, though, that they could be used in measurements for the investigation of processes leading to the enrichment or depletion of implantant at the surface, and which, therefore, are of consequence for certification of reference materials.

5. THE DEPTH DISTRIBUTION OF AN IMPLANTANT

If the retained dose density is known, at least three more pieces of information (called **descriptors** in the following) are required for certification of the concentration-vs-depth profile if the profile is of a symmetrical type (i.e. symmetrical with respect to the depth of the concentration peak), while five descriptors are required if the profile is of an asymmetrical type. For a symmmetrical profile the descriptors required are (1) a depth location parameter, (2) a scale parameter, and (3) a statement as to the functional (i.e. mathematical) form of the profile; these can be (1) the centroid depth, (2) the coefficient of variance, and (3) the statement that the profile is Gaussian (say). For an asymmetrical profile the descriptors can be (1) the centroid depth, the coefficients of (2) variance, of (3) skewness and of (4) kurtosis, and (5) the statement that the profile is of the Pearson IV type (say). An alternative set of five descriptors will be recommended below.

As a rule, implantant profiles are asymmetrical, and, also as a rule, the exact functional form of the **as-implanted** (i.e. the true) profile is unknown. Instead, we have **as-measured** depth profiles, Monte-Carlo-simulated (i.e. theoretical) depth profiles, and other theoretically derived descriptor values. The as-measured profiles consist of convolutions of the as-implanted profile with various broadening and displacement functions introduced by the analytical technique. In other words, the as-measured profile usually is broader and deeper then the as-implanted profile. The simulated profiles and the theoretical descriptor values depend on the ansatz used and on the (usually simplifying) assumptions made for computation. In theoretical work, many of the processes which add to (rather than dominate) the final as-implanted profile are insufficiently treated. As a result, the theoretical information pertains to a profile which should be narrower and shallower than the as-implanted profile if correct input data are being used. Since the average analyst is not in a position to verify compliance with the latter condition other than by comparison with as-measured results, the general rule should be: Do not trust a theoretical descriptor value if it pertains to a profile which is broader and/ or deeper than a carefully measured and correctly scaled profile. Even this simple rule is difficult to apply, though, because the correct scaling of an as-measured profile is a major problem, in general. Thus, the difficulty faced in certification is to derive a most likely as-implanted profile from non-representative information loaded with unknown error margins.

In the following, some of the difficulties are sketched which face both the theoretician and the analyst, and a procedure is proposed which promises to lead to acceptable approximations to as-implanted profiles.

As-implanted profiles are the result of two stopping processes (so-called ´nuclear´ and ´electronic´ stopping), of target-related effects, and of after-effects on the implantant atom once it has come to a stop. The target-related effects include property modification of the target during implantation (amorphization, re-crystallization, stoichiometry change, and other), surface displacement and roughening due to sputtering, and effects due to the fact that the surface is a discontinuity which, moreover, is overlaid by a native oxide layer. The phenomenon known as channeling is also a target-related effect which occurs in crystalline targets if the direction of ion incidence coincides with a major ´open´ crystallographic axis and if, therefore, a significant fraction of the ions is ´channeled´ deep into the target. After-effects on a captured implantant atom comprises all effects which lead to the subsequent removal from the site of initial rest; it includes recoil ejection (due to direct or indirect kinetic energy sharing with later arriving ions), diffusion (of the implantant atom relative to its neighbouring target atoms), and sputtering. All of the above effects would have to be part of a theoretical treatment for a realistic prediction of the as-implanted profile. Most treatments fall far short of this requirement. Any attempt at such a treatment soon faces the problem that most of the input information required is either unavailable or not sufficiently accurate.

At this stage it is appropriate to reflect on the data presented in section 4 and on the reliability of the input data used: The profile descriptor values were taken from tables known to have been generated by theoretical treatments,

free of any target-related effects and after-effects. Hence, the profile depths and widths used may be too small in a number of cases, in which significant target-related effects and/or after-effects occur. Of the effects mentioned above, only (1) underestimated sputter yields and (2) effects which lead to a significant broadening of the profile will give rise to overestimates of the limiting dose density d_a^1. The sputter yield data are semi-empirical and, hence, are realistic. Of the profile-broadening effects, diffusion is both the most significant and the most unpredictable. The reason is that the activation energy for diffusion is strongly affected by radiation damage in the target and very little data is available on activation energy under implantation conditions. Presently, the surest way to discover significant diffusion is to compare predicted and as-measured profiles. In conformity with the assumption of theory (see below) the target should then be amorphous prior to implantation.

For certification of an as-implanted profile one faces the dilemma of having to fall back on the same analytical technique which the certified reference material is intended for, viz. secondary ion mass spectrometry (SIMS). SIMS is the only technique featuring the extreme limits of detection (down to ppb) required for achieving a sufficient dynamic range for determination of an implantant profile in a semiconductor host. The dynamic range is considered sufficient if it extends over four orders of magnitude, i.e. down to 10^{-4} of the peak concentration. On analysis by SIMS the as-implanted profile is subjected once again to certain of the target-related effects and all of the after-effects mentioned in connection with the implantation. Additionally, instrument broadening functions are convoluted-in.

There are very few analytical techniques which can be expected to leave the as-implanted profile unchanged and which, at the same time, feature acceptably narrow instrumental broadening functions, such that a profile-related information, which any of the techniques may be capable of providing, could be considered as representative of the as-implanted profile. There are three techniques which qualify sufficiently well for the provision of at least one profile descriptor value of an as-implanted profile, viz. the centroid depth. These techniques are angle-resolved x-ray fluorescence spectrometry (AR/XFS) (refs. 14, 16, 30), angle-resolved electron microbeam analysis (AR/EMA) (ref. 18), and Rutherford backscattering spectrometry (RBS). While RBS is a well-established and well-documented technique, the angle-resolved techniques are rather recent developments which have not yet attained their full potential. Even though, it can be stated that AR/XFS stands out among the three for the properties: No damage to the sample, well-understood physics of excitation and signal attenuation, quantitative results at the 10^{14} cm^{-2} dose density level (if synchrotron radiation is used), and applicability to a large number of implantant/target combinations. With AR/EMA quantitative results can be obtained at the 10^{16} cm^{-2} dose density level for somewhat fewer implantant/target combinations, and at the danger of damaging the sample by action of the electron beam. Although AR/XFS and AR/EMA can be used to validate profile shape information, neither technique is capable of full profile reconstruction from experimental data. In contrast, RBS measurements yield the profile shape, but only over a rather limited dynamic range and with considerable uncertainty on the deep side (due to the phenomenon known as 'straggling'). The deterioration of the RBS depth resolution to > 10% of depths in excess of 100 nm does not allow the extraction of accurate values of mode, centroid depth or variance for deep implants. Problematic is also the fact that RBS is an ion beam technique, which is bound to cause radiation damage and implantant displacement (though at a low level) in addition to depositing hydrogen (from the probing beam).

Now to the sources and nature of the theoretical information. The sources fall into three groups: (1) transport theory, (2) Monte Carlo (MC) codes, and (3) sampling theory. Most models generate information on the probability density function of the depth penetration of a swift ion/atom of the implantant in a non-ordered host material. It is commonly assumed that this probability density distribution can be equated to the depth distribution of an infinitesimal dose density of implantant in an amorphous target, despite the fact that there may be considerable differences between the model of the target and the actual amorphous state. This should be kept in mind if the validity of a model is

checked by experiment on an "amorphous" target, although there is little alternative to this practice. (Note: The amorphous state is still ill-understood. It can be described as a state of maximum disorder in a dense solid. In a surface layer of a monocrystalline semiconductor wafer this state can be attained by ion bombardment. According to a **rule-of-thumb** the dose density required is that which causes about two atomic monolayers to be sputtered. Infrared luminescence microscopy on ion-bombarded GaAs has shown the disorder corresponding to this rule to be 80 to 90% of maximum - ref. 38.)

Transport theory (ref. 31) yields lower order moments of this depth distribution, without, however, providing the functional form. The moments are calculated as if the surface were only a starting plane for the ions inside an infinite solid. Hence, surface effects are not included in the treatment. Both nuclear and electronic stopping are considered. The moments are calculated using stopping power values derived from assumed interaction potentials. Biersack and Ziegler (ref. 31) estimate the accuracy of these stopping power values to be within a factor of two for the energy range < 200 keV/amu. They estimate the first moment values to be more accurate than this, the higher moments to be less accurate. This is important to remember when comparing the moments of experimental profiles with theoretical moments. Most tables provide the first two moments only (i.e. the centroid depth and the variance), none more than the first four (i.e. centroid depth, variance, skewness and kurtosis). Four or fewer moments do <u>not</u> uniquely define the functional form of the depth distribution (even if these moments were known to a high accuracy). Functions of the Pearson IV type became much-favoured fitting functions (ref. 32) for general use on implantants, and, hence, also for theoretical profile generation, after Hofker (ref. 33) used these functions for SIMS-measured concentration profiles of boron in silicon. It must be emphasized again, though, that the use of these functions is purely arbitrary.

Monte Carlo codes (ref. 34) provide a complete profile in histogram form, inclusive of surface effects. The ion is started with full energy at the surface and the trajectory is followed from elastic binary collision to elastic binary collision (i.e. nuclear stopping) on assumption of a random arrangement of target atoms. Electronic stopping is accounted for by adding a continuous loss of energy due to "friction" in the internuclear electron "sea". In the simplest version the target is treated as virgin for each ion trajectory calculated, when the MC code yields a histogram of the depth penetration probability density rather than one of a concentration profile. In more sophisticated versions, the incorporation of earlier arriving implantant is considered and (zero-order) concentration profile histograms are calculated. Codes have also been developed which allow target-related effects (such as channeling) and/or certain after-effects to be considered; most of these codes are either proprietary, insufficiently documented, or at the experimental stage. The moments of the depth distribution histogram can be calculated with as much accuracy as the statistical error on the histogram bars at the lower concentrations will permit. In order for this statistical error to be acceptably small at the lowest of a four orders of magnitude dynamic range, a total of several 10^6 trajectories have to be calculated. This requires the use of powerful computers. No systematic study appears to have been published which would allow conclusions to be drawn either on the general functional form of the depth distribution histograms or from a comparison with experimental results.

Sampling theory is presently the only theory which allows direct predictions to be made regarding the functional form of the depth distribution. On the basis of an ansatz for nuclear stopping in an amorphous target and separate consideration of electronic stopping it was concluded that an implantant profile should be representable by a split Student-t function (refs. 35, 17). Meanwhile, split Student-t functions have been found (refs. 17, 19) to fit many experimental depth profiles as well as MC histograms. This has encouraged the use of these functions in comparative investigations of theory and experiment. Besides the fact that, in contrast to the Pearson IV function, the split Student-t function is retracable to binary collision physics, there are other practical advantages of using the latter rather than the former. In order to appreciate this fact, one has to realize that the family of Student-t functions is an infinite set of symmetrical functions fully specified by and ordered

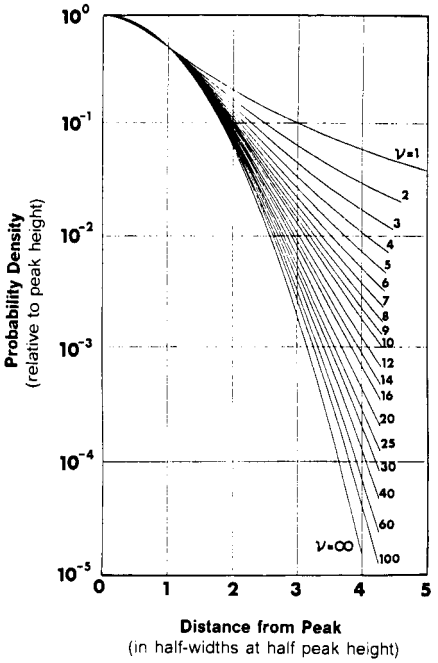

Fig. 9: A sub-set of half Student-t functions to a logarithmic ordinate scale, with the "degree of freedom" shape factor ν as parameter. The bracketing functions with ν = 1 and ν = infinity are identical to the Cauchy and Gauss functions respectively.

according to an integer shape parameter ('degree of freedom', ν) ranging from unity to infinity. A sub-set of these functions (actually only the halves on the positive abscissa) is shown in Fig. 9. An asymmetrical implantant profile can be fitted by a half-function of shape ν_s on the shallow side, and by a half-function of shape ν_d on the deep side. Both halves are joined at the distribution mode (i.e. the depth of peak). On an absolute depth scale a split Student-t function can be fully specified by the use of five parameters which are readily associated with prominent features of the function, viz. the mode, the two shape parameters ν_s and ν_d , and two corresponding scaling factors such as the half-widths at half maximum $(HWHM)_s$ and $(HWHM)_d$. Pearson IV functions, in contrast, require the four moment parameters centroid depth, variance, skewness and kurtosis for a complete description, i.e. parameters which are not readily associated with the prominent features of an asymmetrical profile.

In view of the above, it is concluded that the determination of an as-implanted profile is possible only by reconstruction using (1) indirect evidence as to the shape from theory and from as-measured profiles, and (2) direct evidence as to the centroid depth from AR/XFS, AR/EMA and RBS.

6. THE MICROSCOPIC DISTRIBUTION OF AN IMPLANTANT AND THE ANALYTICAL CONSEQUENCES

In section 5 it was pointed out that as-measured profiles determined by SIMS would have to be relied upon to provide decisive information on the shape to be expected for as-implanted profiles. This is possible only on condition that a linear relationship exists between concentration and signal over the complete dynamic range., i.e. from peak concentration down over four orders of magnitude. A key condition is that the implantant/target system is in a dilute state of solution at all depths. In other words, the solubility limit is not to be exceeded and the probability for statistical clustering of implantant atoms has to remain at an acceptably low level. Statistical clustering arises from the spatially random nature of both the ion incidence on the surface and the nuclear stopping process in the target. Because the ionization efficiency is known to be affected by the nature of the chemical bonding between the sputtered ion and its neighbours (at the instant of sputtering), clustering of implantant atoms is bound to change the chemical bonding and, hence, must affect the linearity between the average concentration at a given depth and the SIMS signal arising therefrom. While it may be argued that a dimer (double cluster) may not be significantly affected in the presence of five other neighbours in a simple

cubic lattice, it would be safe to assume that the same cannot be said for a triple cluster or any higher order cluster. Hence, on the assumption that the fraction of atoms involved in triple clusters causes a corresponding fractional change in signal, a **rule-of-thumb** can be formulated which calls for the fraction of atoms involved in triple clustering to remain below 1% (say) if the linearity is to stay, likewise, within an error margin of 1%. The corresponding critical average concentration can be calculated by means of the binomial probability function

$$P_N(n,c) = \{ N! / [n! (N - n)!] \} c^n (1 - c)^{N-n} \qquad (5)$$

where P is the probability of finding n implantant atoms among a total of N atoms surrounding a given implantant atom, if the average atomic concentration of implantant is c. For a co-ordination number N = 6 (i.e. a simple cubic lattice) and a probability for triple clustering $P_6(2,c) = 0.01$, the average concentration must not exceed $c = 0.027$. Comparison with the peak concentration values in Table 5*a* shows this critical average concentration to be exceeded in some cases if a dose density of 10^{15} cm^{-2} is applied (see also section 4.5.1).

7. CLASSIFICATION AND CERTIFICATION OF ION-IMPLANTED REFERENCE MATERIALS: AN OUTLOOK

Under the auspices of VAMAS (see introductory section) a project is underway for the preparation and certification of ion-implanted reference materials, targeted (initially) for application in SIMS analysis of semiconductor wafers. A concept has been drafted (ref. 1) which accommodates both the widely divergent material requirements of analysts and the high demands on certification with emphasis on economy of effort and cost. The salient features of the concept are sketched as an outlook:

Essentially there will be three classes of reference materials, viz. **primary, secondary and working reference materials** (abbreviated PRM, SRM and WRM in the following). Tables 6*a* and 6*b* pertain. The WRM is the analyst's workhorse for which he (1) supplies the host material and (2) orders the implantation to be made according to his requirements. This implanted material is calibrated - to an accuracy specified by the analyst - against a certified SRM and in accordance with a recommended non-destructive calibration procedure. The techniques of AR/XFS and AR/EMA feature prominently in these calibration procedures. The SRM are also ion-implanted reference materials, which are intented to transfer the certified properties from PRM to WRM. The SRM are certified and provided by a central organization which is to be responsible also for the preparation, certification and upkeep of the PRM. The SRM are calibrated against the PRM by essentially the same non-destructive calibration procedure as used for the WRM. The PRM are certified to the highest accuracy possible, which entails that the PRM be prepared by quantitative ion implantation. The non-destructive procedure for calibration of the SRM ensures that the same PRM can be used over and over again. Hence, the effort of certification of the PRM must be made once and the cost can be spread over many SRM.

8. SUMMARY AND CONCLUSION

In the above critical evaluation it has been shown that the preparation and certification of ion-implanted reference materials is not as straight-forward as is often suggested and believed. The information presented should enable the analyst to specify and query conditions of ion implantation and certification in accordance with his particular requirements. This information includes *inter alia* sputtering yields, conditions for quantitative ion implantation, limiting dose densities for quantitative ion implantation, current understanding of depth distributions, differences between theoretical, as-implanted and as-measured depth distributions, concentrations at the distribution maximum and at the surface, critical concentrations for depth profiling by SIMS, supported by user-friendly graphs, tables, formulas and rules-of-thumb. The data cover implantants (analytes) and host materials with atomic numbers (Z_1 and Z_2 respectively) between 10 and 80 (with the proviso $Z_1 \geq Z_2$), in the energy range 10 to 300 keV.

Table 6a. Classification of ion-implanted reference materials

reference material	host	certification
primary (PRM)	Si	absolute
secondary (SRM)	Si	dose density relative to PRM
working (WRM)	as required	dose density relative to SRM

Table 6b. Properties to be certified and proposed certifying techniques

property	certifying technique
retained dose density	PRM: quantitative ion implantation nuclear activation analysis Rutherford backscattering spectrometry SRM & WRM: x-ray fluorescence spectrometry (XFS) electron microbeam analysis (EMA)
depth distribution shape	secondary ion mass spectrometry Rutherford backscattering spectrometry angle-resolved XFS angle-resolved EMA *in combination with* Monte Carlo simulation transport theory sampling theory
centroid depth	angle-resolved XFS angle-resolved EMA Rutherford backscattering spectrometry
surface roughness	Nomarski microscopy atomic force microscopy scanning electron microscopy
oxide skin thickness	various

A self-consistent nomenclature is proposed which is aimed at improving the precision of communication between analyst and implanter technologist and, hence, at avoiding misconceptions about ion-implanted reference materials and the possible misinterpretation of measured data.

Certification has been shown to be an exercise best undertaken in concerted international action such as is presently underway within the VAMAS project. It holds out the prospect of traceability for all secondary and working reference materials to one set of carefully certified primary reference materials.

REFERENCES

1. W.H. Gries, J. Vac. Sci. Technol. A7 , 1639 (1989).
2. e.g. G. Larrabee and R. Dobrott, Report NBS-GCD-79-158, National Bureau of Standards, Washington D.C. 20234, 1979.
3. e.g. D.P. Leta and G.H. Morrison, Anal. Chem. 52 , 514 (1980).
4. W.H. Gries and W.L. Rautenbach, Preprints 6th Int. Symp. Micro-techniques, Verlag der Wiener Medizinischen Akademie, Vienna, vol.E , p.83 (1970).
5. W.H. Gries and E. Norval, Anal. Chim. Acta 75, 289 (1975).
6. W.H. Gries, Proc. 7th Int. Vac. Congr. and 3rd Int. Conf. on Solid Surfaces, R. Dobrozemski, F. Rüdenauer, F.P. Viehböck, and A. Breth (eds.), Postfach 300, A-1082 Vienna, p. 1425 (1977).
7. W.H. Gries, Nucl. Instr. Meth. 152, 453 (1978).
8. W.H. Gries and J. Steyn, Nucl. Instr. Meth. 152, 459 (1978).
9. W.H. Gries, Int. J. Mass Spectrom. Ion Phys. 30, 97 (1979).
10. W.H. Gries, Int. J. Mass Spectrom. Ion Phys. 30, 113 (1979).

11. W.H. Gries and F.T. Wybenga, X-Ray Spectrom. 8, 175 (1979).
12. W.H. Gries, Nucl. Instr. Meth. 189, 287 (1981).
13. W.H. Gries, Mikrochim. Acta (Wien) 1981 I, 335.
14. W.H. Gries and F.T. Wybenga, Surf. Interface Anal. 3, 251 (1981).
15. W.H. Gries, Mikrochim. Acta (Wien) 1985, Suppl. 11, 33.
16. W.H. Gries, Fresenius Z. Anal. Chem. 329, 133 (1987).
17. W.H. Gries, Mikrochim. Acta (Wien) 1990 II, 55.
18. W.H. Gries and W. Koschig, Surf. Interface Anal. 16, 321 (1990).
19. W.H. Gries, unpublished.
20. J. Uhler, Arkiv f. Fysik 24, 329 (1963).
21. J. Uhler and J. Rossi, Arkiv f. Fysik 24, 369 (1963).
22. D.E. Sykes and R.T. Blunt, Vacuum 36, 1001 (1986).
23. J.H. Freeman, D.J. Chivers and G.A. Gard, Nucl. Instr. Meth. 143, 99 (1977).
24. W. Eckstein and J.P. Biersack, Z. Phys. B - Condensed Matter 63, 471 (1986), and W. Eckstein, Report IPP 9/61, Max Planck Institute f. Plasma Physics, Garching, 1987.
25. W.H. Gries and H.J. Strydom, Report SMAT 3, Nat. Inst. Mater. Res. / CSIR, Pretoria (South Africa), 1984.
26. H.J. Strydom and W.H. Gries, Rad. Eff. Lett. 86, 145 (1984).
27. P. Sigmund, Phys. Rev. 184, 383 (1969).
28. R. Hultgren, P.D. Desai, D.T. Hawkins, M. Gleiser, K.K. Kelly and D.D. Wagman, Selected Values of Thermodynamic Properties of the Elements, American Society of Metals, 1973.
29. B. J. Smith in: G. Dearnaly, J.H. Freeman, R.S. Nelson and J. Stephen, Ion Implantation, North-Holland, Amsterdam and London, 1973.
30. W.H. Gries, J. Vac. Sci. Technol. A7, 1655 (1989).
31. J.P. Biersack and J.F. Ziegler in: Ion Implantation Technique (eds. H. Ryssel and H. Glawischnig), Springer Series in Electrophysics 10, Springer-Verlag, Berlin, 1982.
32. H. Ryssel in: Ion Implantation Technique (eds. H. Ryssel and H. Glawischnig), Springer Series in Electrophysics 10, Springer-Verlag, Berlin, 1982.
33. W.K. Hofker, Philips Res. Reports, Suppl. 8, (N.V. Philips, Eindhoven, Netherlands), 1975.
34. e.g. O.S. Oen and M.T. Robinson, Nucl. Instr. Meth. 132, 647 (1976).
35. W.H. Gries, Quantitative Ion Implantation, (Ph.D. thesis), Univ. Stellenbosch (South Africa), 1976.
36. L.A. Larson, J. Electrochem. Soc.: Solid-State Science and Technology 135, 1802 (1988).
37. M.I. Current and W.A. Keenan, Nucl. Instr. Meth. Phys. Res. B6, 418 (1985).
38. O. Hoinkis, K. Miethe, W. Betz and W.H. Gries, Fresenius J. Anal. Chem. 341, 101 (19919.

APPENDIX 1: TERMINOLOGY RELATED TO BEAMS AND ION IMPLANTATION

TERMINOLOGY RELATED TO BEAMS

Introductory remark: In ion implantation, the quantification of the implantant in the target is largely determined by the quality of the beam in which ions of the implantant are transported to the target (where 'implantant' is 'that which is to be implanted'). Hence, the beam must be described by an appropriate terminology.

1. Particles in a beam

1.1 **heavy particle**
an electrically charged or uncharged atom, molecule or other atom cluster.

1.2 **ionic particle**
an electrically charged heavy particle.

Synonymous terms: ion, charged heavy particle.

1.3 **neutral particle**
an electrically uncharged heavy particle.

Synonymous terms: neutral heavy particle, neutral.

1.4 **drift electron**
an electron travelling in a beam of positive ions

2. Particle fluxes in a beam

2.1 **heavy-particle flux**
the number of heavy particles within a beam passing per unit time.

2.2 **ionic-particle flux**
the number of ionic particles within a beam passing per unit time.

Synonymous term: ion flux.

3. Particle flux densities in a beam

3.1 **heavy-particle flux density**
the number of heavy particles incident per unit time on a small sphere, divided by the cross-sectional area of that sphere.

Note:
This definition is analogous to that for 'particle flux density' in the nuclear field as adopted by ISO (ISO 31/10-1980).

3.2 **ionic-particle flux density**
analogous to 3.1

Synonymous term: ion flux density.

4. Fluences in a beam

4.1 **heavy-particle fluence**
the integral over time of the heavy particle flux density (cf. 3.1).

Note: This definition is analogous to that for 'particle fluence' in the nuclear field as adopted by ISO (ISO 31/10-1980).

4.2 **ionic-particle fluence**
analogous to 4.1

Synonymous term: ion fluence.

5. Quantities of electric charge in a beam

5.1 **ionic current**
the electric charge carried by heavy particles within a beam passing per unit time.

Synonymous term: ion current.

5.2 **drift-electron current**
the electric charge carried by drift electrons passing per unit time in the foreward direction of the ions.

5.3 **net beam current**
the excess of the positive ionic current over the drift electron current.

6. Constituents in a beam

6.1 **nominal constituent**
the set of identical heavy particles of implantant (in a beam).

6.2 **incidental constituent**
the set of drift electrons or a set of identical heavy particles other than implantant (in a beam).

7. Types of beam

7.1 **total beam**
a beam consisting of nominal and incidental constituents prior to separation.

7.2 **nominal beam**
a separated beam in which the nominal constituent is the major constituent.

7.3 **incidental beam**
analogous to 7.2

TERMINOLOGY RELATED TO BEAM MEETING TARGET

Introductory remark: In ion implantation, some beam-related quantities loose their meanings at incidence of the beam. For instance, ionic particles change their state of charge; hence, the attribute 'ionic' loses its meaning. A primary concern in ion implantation is the quantification of the implantant. Hence, particle flux density in a beam is of interest only if it pertains to a (uniform) broad beam applied stationary; it bears no relationship to the lateral density of implantant if the beam is scanned. In the latter case, the size of the area of incidence is of cardinal importance. The tilt of the area of incidence is of importance in either case. These facts demand a terminology appropriate for the incidence and subsequent fate of the nominal constituent of the beam.

8. Quantities of electric charge incident on a surface

8.1 **on-surface ionic charge** (Q_i)
integral over time of the ionic current incident on a surface.

Synonymous term: received ionic charge.

8.2 **on-surface net electric charge** (Q)
integral over time of the net beam current incident on a surface.

Synonymous term: received net electric charge.

8.3 **on-surface ionic-charge density** (area-averaged) (q_i)
the on-surface ionic charge, divided by the geometric area of incidence.

Synonymous term: received ionic charge density.

Note: The geometric area is the area on a mathematical plane and is to be distinguished from the surface area, which may be larger due to roughness.

8.4 **on-surface net-electric-charge density** (area-averaged) (q)
analogous to 8.3

Synonymous term: received net electric charge density.

9. Quantities of particles incident on a surface

9.1 **on-surface heavy-particle flux density**
the number of heavy particles incident per unit time on a small area on the surface, divided by the geometric area.

Equivalent definition: integral over time of the heavy-particle flux density at the area of incidence, multiplied by $\cos \alpha$, where α is the angle between the direction of incidence and normal incidence.

9.2 **on-surface ionic-particle flux density**
analogous to 9.1

Synonymous term: on-surface ion-flux density.

9.3 **on-surface heavy-particle dose** (D)
integral over time of the heavy-particle flux incident on a surface.

Synonymous term: received heavy-particle dose.

9.4 **on-surface ionic-particle dose** (D_i)
analogous to 9.3

Synonymous terms: received ionic-particle dose, received ion dose.

9.5 **on-surface heavy-particle dose density** (area-averaged) (d)
the on-surface heavy-particle dose,
divided by the geometric area of incidence.

Synonymous term: received heavy-particle dose density.

Note: This definition applies equally for stationary and scanned beams.

Equivalent definition for broad stationary beams: integral over time of the on-surface heavy-particle flux density.

Synonymous terms for broad stationary beams: on-surface heavy-particle fluence, received heavy-particle fluence.

9.6 **on-surface ionic-particle dose density** (area-averaged) (d_i)
analogous to 9.5

Synonymous terms: received ionic-particle dose density, received ion-dose density.

Note: This definition applies equally for stationary and scanned beams.

Equivalent definition for broad stationary beams: analogous to 9.5

Synonymous terms for broad stationary beams: on-surface ionic-particle fluence, on-surface ion fluence, received ionic-particle fluence, received ion fluence.

10. Quantities of an implantant passing into a target

Introductory remarks: On passing into a target, the distinction between 'ionic' and 'heavy' particles falls away. The received heavy-particle dose splits into two fractions; one, consisting of implantant particles which are fully slowed down and become trapped, and another, consisting of implantant particles which are re-emitted before becoming trapped. The former fraction may suffer losses by sputtering of the target during the process of implantation.

10.1 **implanted dose** (D^{im})
the fraction of the on-surface heavy-particle dose
trapped in the target.

10.2 **implanted-dose density** (d^{im})
the fraction of the on-surface heavy-particle dose density
trapped in the target.

Note: This definition ignores the lateral spreading of the particles in the target, i.e. 'density' here implies (areal) density at incidence.

10.3 **non-implanted dose** (D^{nim})
the fraction of the on-surface heavy-particle dose
not trapped in the target.

10.4 **non-implanted dose density** (d^{nim})
the fraction of the on-surface heavy-particle dose density
not trapped in the target.

10.5 **sputtered dose** (D^{sp})
the fraction of the implanted dose lost by sputtering.

10.6 **sputtered-dose density** (d^{sp})
the fraction of the implanted-dose density lost by sputtering.

10.7 **retained dose** (D^{ret})
the fraction of the implanted dose remaining in the target.

10.8 **retained-dose density** (d^{ret})
the fraction of the implanted-dose density remaining in the target.

APPENDIX 2: ION DOSIMETRY IN TECHNOLOGICAL IMPLANTERS

As was made clear in the main text, in-situ ion dosimetry in ion implanters can be regarded as a direct means of measurement of the retained dose density of implantant only under the exceptional conditions prescribed for quantitative ion implantation. These conditions are not normally met in implantations undertaken in technological ion implanters; in short, the dose density quoted for an implant is not the same as the retained dose density required by the analyst. While this fact is readily apparent from the present report, it is useful to have some data in hand on the reproducibility (as distinct from repeatability and accuracy) of dose density figures. The reproducibility can be derived from the results of measurements of the electronic activities (measured as resistivity values) induced in ion-implanted silicon wafers as obtained in various round robin exercises. Here, the reasonable assumption is made that, at least for low dose densities, the resistivities measured are directly proportional to the retained dose densities .

In a round robin conducted in 1987 (ref. 36), 'on-surface ionic particle dose densities' (measured as 'area-averaged on-surface net-electric-charge densities', called 'doses' in ref. 36) of prescribed values in nominally identical silicon wafers were subjected to resistivity measurements. The prescribed dose densities of 3×10^{13} and 3×10^{15} cm^{-2} boron as well as 3×10^{15} cm^{-2} arsenic implanted at 80 keV into a total of 139 wafers in 47 different machines at 15 different production lines were found to give rise to resistivities featuring standard deviations of 5.8%, 7.0% and 4.9% respectively about the corresponding mean values, and this after 8 wafers (i.e. 5% of the total) had been excluded as "obviously mis-implanted". Analysis of the data also showed systematic deviations related to the type of machine. The largest difference between the averages of any two types was 8.5%. The largest standard deviation on one particular type was also 8.5%.

Other round robin results provide a similar to less favourable picture. For instance, Current and Keenan (ref. 37) report standard deviations of 14.3%, 12.9%, 6.5% and 6.4% respectively for the resistivity values measured on 34, 33, 34 and 14 wafers implanted at 80 keV with nominally 5×10^{13}, 5×10^{14}, 5×10^{15} and 1×10^{16} cm^{-2} arsenic respectively. Again type-to-type differences were found as well as machine-to-machine differences for a given type; the former up to 13.4% difference between type averages, and the latter 8.8%, 6.5% and 4.0% standard deviation respectively for the low, medium and high dose densities. While the results in ref. 37 show an improvement of dosimetry with increasing dose density, five earlier round robins (referred to in ref. 37) show the opposite, viz. the dosimetry worsens at higher dose densities.

It can be concluded that ion dosimetry in technological ion implanters is not sufficiently reliable (i.e. neither accurate nor reproducible) for providing retained dose density values for ion-implanted reference materials.